

# Isotherm and kinetics modeling of Pb(II) and Cd(II) adsorptive uptake from aqueous solution by chemically modified green algal biomass

Tabrez Alam Khan<sup>1</sup> · Amer Arif Mukhlif<sup>1</sup> · Equbal A. Khan<sup>2</sup> · Durlubh K. Sharma<sup>3</sup>

Received: 23 May 2016 / Accepted: 4 June 2016 / Published online: 23 June 2016  
© Springer International Publishing Switzerland 2016

**Abstract** In this study, the adsorption efficiency of epichlorohydrin modified fresh water green algal biomass was assessed for Pb(II) and Cd(II) uptake from aqueous solution. The process parameters such as contact time, dose, initial metal concentration, solution pH and temperature were optimized. The Langmuir, Freundlich, Temkin and Dubnin–Redushkevich isotherm model was applied to the equilibrium data, which best fitted the Langmuir isotherm indicating homogenous distribution of adsorption sites. The monolayer adsorption capacity was 100.00 for Pb(II) and 72.46 mg/g for Cd(II) adsorption. The kinetic data was best described by pseudo-second order model, with intraparticle and liquid film diffusion controlled mechanism. The negative values of Gibbs free energy change ( $\Delta G^\circ$ ) and positive enthalpy change ( $\Delta H^\circ$ ) showed that adsorption process was spontaneous and endothermic. The functional groups, surface morphology and elemental composition of adsorbent, before and after adsorption, was evaluated using FTIR spectra, SEM and EDS studies. The study revealed that the modified algal biomass can effectively and efficiently remove the title metal ions from aqueous solution.

**Keywords** Epichlorohydrin modified green algae · Pb(II) · Cd(II) · Langmuir · Pseudo-second order

## Introduction

The aquatic contamination due to discharge of industrial wastewater containing toxic and non-biodegradable metals, which tend to traverse through the food chain is causing severe physiological or neurological damage to human and aquatic system (Mohan and Sreelakshmi 2008). The wastewaters generated from electroplating, NiCd batteries, smelting, mining and refining process, and plastics are major sources of cadmium(II) contamination. Lead(II) is released into the aqueous streams by printing, lead smelting and mine tailings, lead batteries and glass manufacturing industries. Human exposure to Pb(II) and Cd(II) above the permissible limits (0.005 mg/L for Pb<sup>2+</sup> and 0.015 mg/L for Cd<sup>2+</sup> (USEPA, 2009) are potentially toxic and may cause kidney and liver damage, decrease in hemoglobin formation, infertility, mental retardation, chills, diarrhea, anemia, abnormalities in pregnant women and failure of central nervous system (Khan and Singh 2010; Martins et al. 2004). Consequently, the treatment of effluents containing Pb(II) and Cd(II) is quite imperative. Various treatment techniques such as precipitation (Ku and Jung 2001), electrochemical (Cooper et al. 2007), ion-exchange (Dąbrowski et al. 2004), coagulation/electrocoagulation (Ali et al. 2012; El-Samrani et al. 2008), and electrodialysis (Sadrzadeh et al. 2008) are rather inept and/or cost prohibitive. Biosorption, using sustainable resources, is considered a promising process due to its high removal efficiency, low cost, mild operating conditions and good performance in the removal and recovery of heavy metal ions/dyes from dilute aqueous solution (Khan et al. 2012, 2014; Lou et al. 2015). Among various wastes biomass for metal removal such as yeast (Göksungur et al. 2005; Han et al. 2006), bacteria (Halttunen et al. 2007; Loaic et al. 1997; Teemu et al. 2008) and fungi (Kapoor

✉ Tabrez Alam Khan  
takhan501@yahoo.com

<sup>1</sup> Department of Chemistry, Jamia Millia Islamia, Jamia Nagar, New Delhi 110 025, India

<sup>2</sup> Department of Chemistry, Al Falah University, Dhauj, Faridabad 121004, India

<sup>3</sup> Center for Energy Studies, Indian Institute of Technology Delhi, Hauz Khas, New Delhi 110 016, India

et al. 1999), algal biomass is favorite adsorbent because of its low cost and widespread abundance (Carlsson et al. 2003; He and Chen 2014). Algal biomass used for adsorptive removal of heavy metal ions from wastewater include green algae ( $\text{Cu}^{2+}$ ,  $\text{Cd}^{2+}$ ,  $\text{As}^{3+}$ ) (Ghoneim et al. 2014; Jayakumar et al. 2015; Tuzen et al. 2009), brown algae (aluminum, molybdenum and rhenium,  $\text{Cd}^{2+}$ ,  $\text{Zn}^{2+}$ ,  $\text{Pb}^{2+}$ ,  $\text{Cr}^{6+}$ ,  $\text{Cu}^{2+}$ ,  $\text{Co}^{2+}$ ) (Akbari et al. 2015; Sar and Tuzen 2009; Lou et al. 2015; Freitas et al. 2008; Javadian et al. 2013), marine green algae ( $\text{Cr}^{6+}$ ) (Jayakumar et al. 2014), dead green algal biomass ( $\text{Cu}^{2+}$ ,  $\text{Zn}^{2+}$ ,  $\text{Cd}^{2+}$  and  $\text{Pb}^{2+}$ ) (Areco et al. 2012), macro algae ( $\text{Cd}^{2+}$ ) (Sarada et al. 2014), red algae (total chromium,  $\text{Cd}^{2+}$ ) (Sar and Tuzen 2008a, b), fresh water algae (cadmium and lead) (Abdel-Aty et al. 2013).

The metal binding capacity of algae depends on the composition of cell wall, which consist of polysaccharides, proteins and lipids containing several functional groups such as  $-\text{COOH}$ ,  $-\text{OH}$ ,  $-\text{NH}_2$ , and  $-\text{SH}$ , which may take part in biosorption (Anastopoulos and Kyzas 2015; Ivánová et al. 2012; Crist et al. 1981). The major active groups for sorption are alginates and sulfates (Anastopoulos and Kyzas 2015). Chojnacka et al. (2005) reported that algal cell wall consists of polysaccharides, proteins peptidoglycan, teichoic acid, teichuronic acid, containing carboxyl, phosphate, hydroxyl or amine groups (Anastopoulos and Kyzas 2015). The red algae cell wall consists of cellulose, but their adsorption capacities is largely because of sulfated polysaccharides made of galactans (Anastopoulos and Kyzas 2015; He and Chen 2014). It has been reported (Montazer-Rahmati et al. 2011) that raw algae has limited applicability in treatment process because of leaching of alginate and other organic constituents from the biomass, which may cause secondary pollution and lower the biosorbent stability. However, chemical surface modification may prevent the leaching of adsorptive components from biomass and increase the stability of the biosorbent (Montazer-Rahmati et al. 2011). Surface modifications of algal biomass using glutaraldehyde, formaldehyde, polyethyleneimine, HCl,  $\text{CaCl}_2$  (Montazer-Rahmati et al. 2011), NaOH (Yang and Volesky 1999), epichlorohydrin and potassium permanganate (Liu et al. 2009) have been reported. The adsorption efficiency of pretreated biomass depend largely upon the nature of chemicals used for modification. The acid treatment open up active sites on the surface (Kratochvil et al. 1998), while treating with  $\text{Ca}^{2+}$  enhance the metal ion exchange ability (Kratochvil et al. 1998). Polyethyleneimine introduces amine group improving the metal binding capacity, whereas NaOH treatment enhance the negative surface charge (Yang and Volesky 1999). Epichlorohydrin treatment increases both stability by crosslinking with carbohydrate in the cell

wall and the adsorption capacity with increase in the hydroxyl groups, which provide the better binding ability with metal ions. Potassium permanganate was used to oxidize marine brown algae *Laminaria japonica* to increase carboxylic groups (Liu et al. 2009), which have been identified as the main metal binding site. Although the adsorption of metal ions using epichlorohydrin modified brown algae (Liu et al. 2009; Montazer-Rahmati et al. 2011) are reported in the literature, the studies on the adsorptive removal of metal ions using epichlorohydrin pretreated freshwater green algae are limited to the best of our knowledge.

In the present work, the removal of Pb(II) and Cd(II) from aqueous solution with epichlorohydrin modified fresh water green algae is reported. Various process variables affecting the adsorption process have been optimized. The isotherm, kinetic and thermodynamic parameters have been evaluated.

## Materials and method

### Materials

The algal biomass was collected from Hauz Khas pond, New Delhi, India.  $\text{Cd}(\text{NO}_3)_2 \cdot 4\text{H}_2\text{O}$ ,  $\text{Pb}(\text{NO}_3)_2$ , cetyltrimethylammonium bromide (CTAB), epichlorohydrin, 2-propanol, dimethylsulfoxide (DMSO) and dithizone (all Merck, India, NaOH and HCl (Fisher Scientific, India) were used as supplied.

### Preparation of adsorbent

The sun-dried algal biomass was washed with double distilled water to remove adhering impurities, oven dried at 50–60 °C, crushed and sieved to 90–120  $\mu\text{m}$  size. Chemical modification was carried out according to Liu et al. (2009). In brief, 100 g of biomass was taken in a 1000 mL tri-necked round bottom flask containing 450 mL of DMSO and vigorously stirred for 24 h at 303 K. Epichlorohydrin (200 mL) was added slowly with stirring for 2.5 h at 293 K. The temperature was increased thereafter to 323 K, followed by addition of 200 mL of NaOH (5 mol/L) and the stirring continued for 5 h. The reaction mixture was allowed to cool to room temperature, filtered using Buchner funnel and washed with aqueous 2-propanol (1:1), HCl (0.5 mol/L) followed by aqueous 2-propanol to remove excess of DMSO and unreacted epichlorohydrin. The washing was continued till the pH of filtrate reached neutral. The resulting treated biomass was finally dried overnight in hot air oven at 333 K, sieved to <75  $\mu\text{m}$  particle size and stored in a polypropylene air tight bottle.

### Preparation of adsorbate solution

The stock solution (100 mg/L) of Cd(II) and Pb(II) was prepared by dissolving 0.2103 g of Cd(NO<sub>3</sub>)<sub>2</sub>·4H<sub>2</sub>O and 0.1598 g of Pb(NO<sub>3</sub>)<sub>2</sub> in double distilled water (1L). The test solutions of different concentrations were prepared by diluting the stock solution.

### Instrumentation

The characterization of the adsorbent, before and after adsorption, was carried out using FTIR spectrometer (400–4000 cm<sup>-1</sup>) (Affinity-1-Simadzu, Japan), and scanning electron microscope, (FEI-Nano-NOVA SEM). Elemental composition was determined by BRUKER SEM with energy dispersive X-ray analyzer attachment (EDX). The adsorbate concentration was determined using a UV-visible spectrophotometer (PG T80+).

### Adsorption experiments

Batch adsorption studies were conducted with algal biomass (15 mg) equilibrated with various concentrations of metal solution (20 mL) for varying contact time (5–120 min) in different stoppered conical flasks (50 mL) in a thermostatic water bath shaker at 303 K between 2 and 10 pH. The aliquots were withdrawn after 10 min intervals using a syringe and the remaining metal concentration was determined colorimetrically using dithizone method at λ<sub>500</sub> for Pb(II) and λ<sub>540</sub> for Cd(II). Initial pHs of the solution was adjusted using 0.1 mol/L NaOH or HCl by using a pH meter (Decibel DB-1011, India). The adsorption capacity (*q<sub>e</sub>*, mg/g) and percent removal of metal ions were calculated using the following Eqs. 1 and 2:

$$q_e = \left[ \frac{(C_o - C_e)}{W} \times V \right] \tag{1}$$

$$\% \text{ Removal} = \left[ \frac{(C_o - C_e)}{C_o} \times 100 \right] \tag{2}$$

where *C<sub>o</sub>* and *C<sub>e</sub>* (mg/L) are the initial and equilibrium concentrations of the metal ions, *V* is the volume of the solution (L), and *W* is the mass of adsorbent (g). All the experiments were performed in triplicate and mean values are reported.

The isotherms studies were performed by shaking 20 mL of metal solution (30–60 mg/L) with fixed adsorbent dose (0.75 g/L) for 60 min at 303–323 K. The kinetic studies were carried out at 10 min interval up to 60 min keeping the dose, initial metal concentration and pH 7 constant.

The adsorption capacity at time *t* (*q<sub>t</sub>*) was estimated by Eq. 3:

$$q_t = [V \times (C_o - C_t)/M] \tag{3}$$

where *C<sub>t</sub>* (mg/L) is the Pb(II) and Cd(II) concentrations at time *t*.

## Results and discussion

### Characterization of adsorbent

#### FTIR studies

FT-IR spectrum of the algal biomass exhibits broad band at 3600-3000 cm<sup>-1</sup> characteristics of –OH and –NH vibrations. The peak at 2920 and 2850 cm<sup>-1</sup> are due to asymmetric and symmetric C–H stretching vibrations, respectively of the alkyl groups. The sharp peak at 1663 cm<sup>-1</sup> is assignable to amide-I bond, and that at 1546 cm<sup>-1</sup> represents the amide-II absorption of the protein fraction (Hu et al. 2014). The peak at 1408 cm<sup>-1</sup> corresponds to deformation vibration of –C–OH with contribution of O–C–O symmetric stretching vibration of carboxylate group. The peak at 1237 cm<sup>-1</sup> is assigned to P=O stretching vibration of phosphate and O–C–O vibration of ester groups. The sharp peak at 1034 cm<sup>-1</sup> is ascribed to carbohydrate fraction (Ferreira et al. 2011). After modification, the peaks at 1408 and 1237 cm<sup>-1</sup> disappear and a new peak at 1383 cm<sup>-1</sup> due to C–O stretching of ether group appears (Fig. 1), which indicates that the carbohydrate moiety in algae is crosslinked with epichlorohydrin.

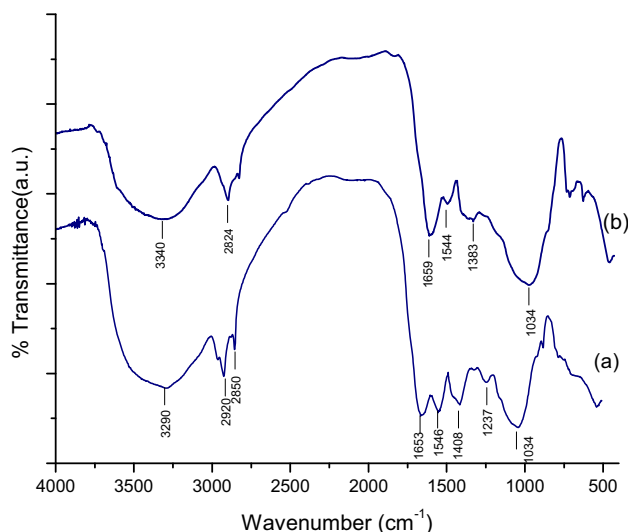


Fig. 1 FTIR spectra of raw (a) and modified algae (b)

### Scanning electron microscopy (SEM) and energy dispersive x-rays (EDX) studies

The SEM images, before and after modification, are shown in Fig. 2. It is evident that after modification the surface becomes more heterogenous and porous due to crosslinking. The smooth surface, after adsorption, is indicative of adsorption of metal ions onto the adsorbent surface. The EDS spectra (Fig. 3) reveal that the algal biomass consists (at %) mainly of C (69.31), and O (17.41), with traces of other elements such as Ca (4.21), Si (3.58), P (1.99), Al (1.21), Fe (0.94), K (0.84), S (0.72), Cl (0.13), Na (0.09), and Mg (0.06). After treatment, the at % changes to C (62.46), O (21.39), S (5.38), Si (2.79), Fe (2.35), Ca (2.06), Cl (1.44), K (0.88), Al (0.71), P (0.41), Na (0.07), and Mg (0.05). The change in at % of Cl may largely be attributed to crosslinking of algal biomass with epichlorohydrin. The EDS spectra of the biomass, after adsorption, shows the

adsorption of Pb (0.07 %) and Cd (0.04 %) on the adsorbent surface.

### Influence of contact time on Pb(II) and Cd(II) adsorption

The effect of contact time on the adsorptive removal of Pb (II) and Cd(II) at 303 K is shown in Fig. 4, which reveals that the percent uptake of metal ions increases rapidly from 58 to 86.8 for Pb(II) and from 53.8 to 80.3 for Cd(II), with no significant increase, thereafter. The equilibrium is achieved at 80 and 60 min for Pb(II) and Cd(II), respectively. About 86.8 and 80.3 % of Pb(II) and Cd(II) is adsorbed at equilibrium time.

### Influence of algal biomass dose

The percentage adsorption of metal ions increases from 75.2 to 89.6 for Pb(II) and from 63.5 to 81.7 for Cd(II) with

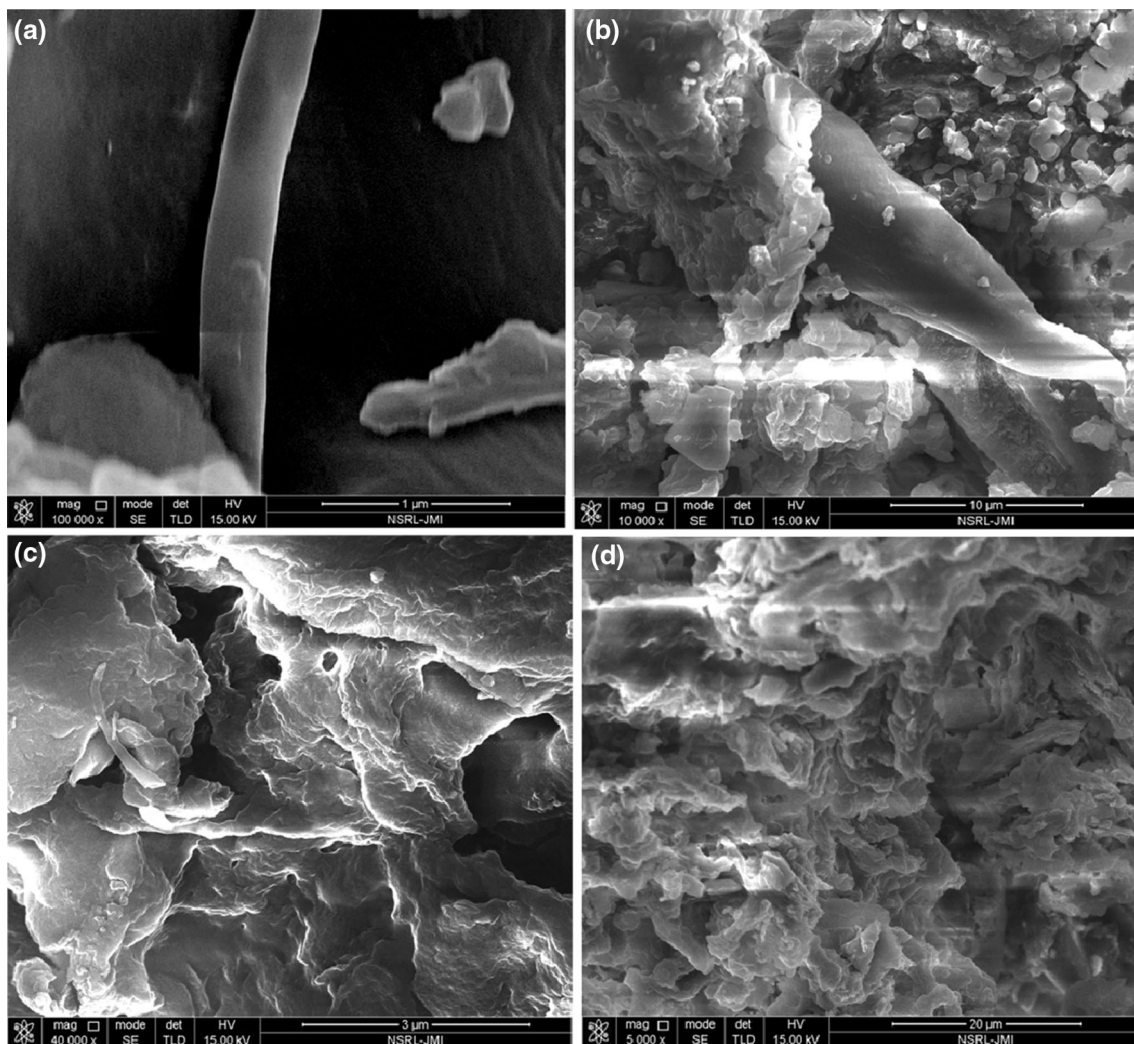


**Fig. 2** SEM images of raw (a), modified algae (b), after Pb (c), and after Cd (d) adsorption



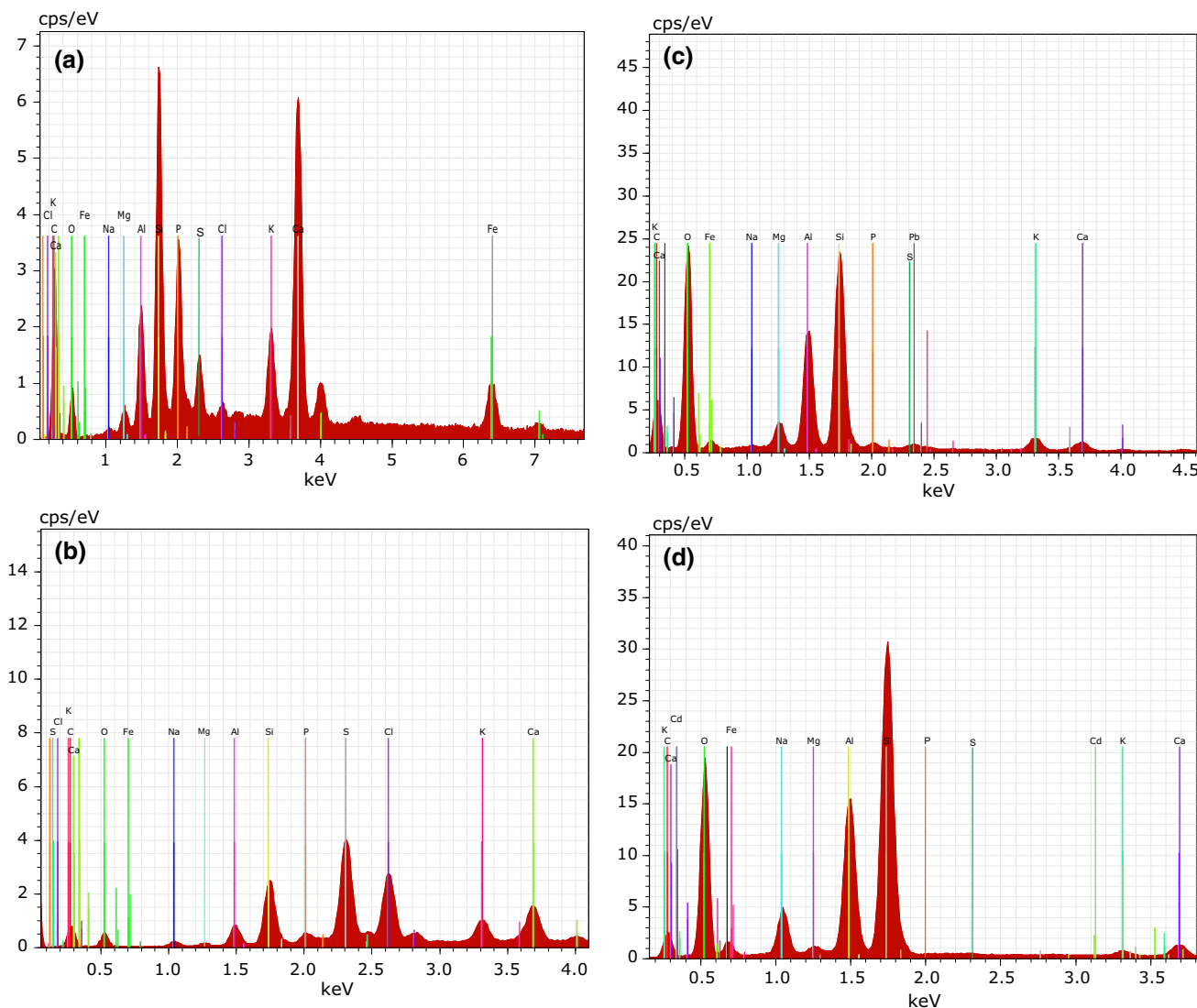


**Fig. 3** EDS spectra of raw (a), modified algae (b), after Pb (c), and after Cd (d) adsorption

increasing adsorbent dose from 0.25 to 1.0 g/L at fixed initial metal concentration (50 mg/L) and equilibrium time (80 min for Pb(II) and 60 min for Cd(II)). However, the adsorption capacity decreases from 151.20 to 44.60 mg/g for Pb(II) and 127.16 to 40.86 mg/g for Cd(II) (Fig. 5). This may be due to increase in the number of available vacant sites with increasing dose resulting in higher removal efficiency. At optimum dose, the adsorption becomes stagnant because of agglomeration of adsorbent and resulting decrease in active sites. The maximum percent removal is achieved at 0.75 g/L adsorbent dose.

*Influence of initial adsorbate concentration*

The initial concentration is considered a vital driving force to overcome all mass transfer resistance of adsorbates between solution and the solid adsorbent. The adsorption of

Pb(II) and Cd(II) onto the adsorbent at optimized adsorbent dose (0.75 g/L) and equilibrium time with varying adsorbate concentrations (30–70 mg/L) at 303 K shows that the percentage Pb(II) and Cd(II) adsorption decrease from 93.3 to 84 % and 92.7 to 81 %, respectively with increasing initial concentration from 30 to 50 mg/L, and remain constant thereafter (Fig. 6). At lower concentration, percentage removal of metal ion is high due to abundance of active sites on adsorbent surface while percent adsorption is almost constant at higher concentration due to non-availability of the surface sites for further adsorption. Equilibrium is achieved at 50 mg/L for Pb(II) and Cd(II) concentration.

*Influence of initial pH*

The extent of adsorption of Pb(II) and Cd(II) on algal biomass largely depends upon the effect of initial solution

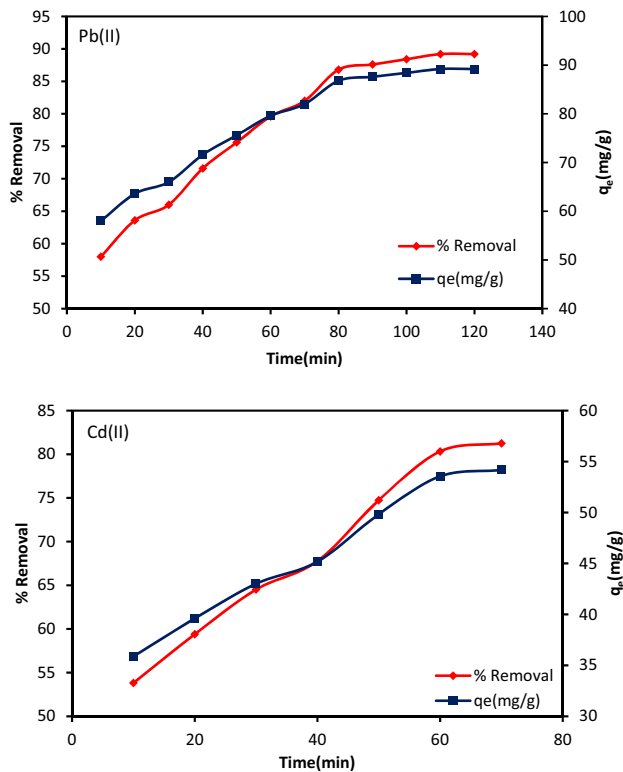


Fig. 4 Effect of contact time

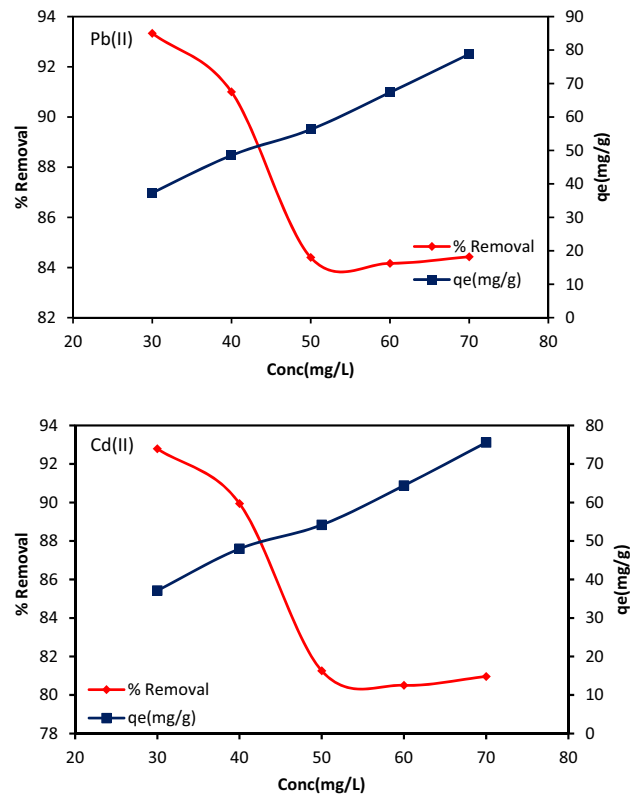


Fig. 6 Effect of Pb(II) and Cd(II) ion concentration

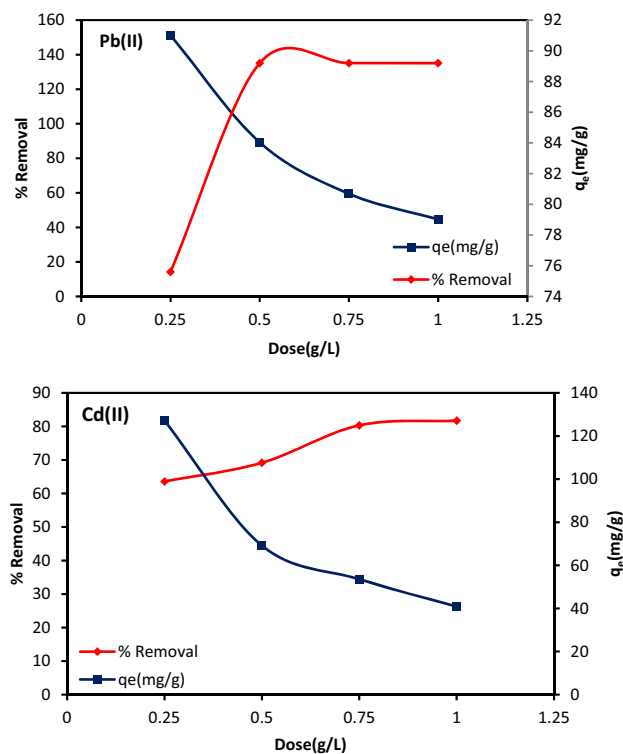


Fig. 5 Effect of algal biomass

pH on the surface adsorption sites and on the speciation of metal ions at different pHs. The percent uptake of Pb(II) and Cd(II) increases from 45.2 to 90.0 and 67.3 to 96.0, respectively with increase in pH from 2 to 10. It has been reported that at lower pH, the metal ion uptake is less because of the  $H_3O^+$  vying with metal ions for the adsorption sites. However, with increasing pH, the surface becomes more negatively charged attracting the Pb(II) and Cd(II) ions, and further increase in solution pH leads to decrease in Pb(II) and Cd(II) concentration due to the formation of  $M(OH)_3$  complex anions ( $M = Pb(II)$  or Cd(II)) resulting in decreased adsorption. Maximum removal of Pb(II) is observed at pH 5 while for Cd(II) it occurs at pH 6 (Fig. 7).

*Influence of temperature and thermodynamic studies*

Temperature is an important parameter affecting the removal of Pb(II) and Cd(II) from aqueous solution. Batch adsorption studies were performed at different temperatures from 303 to 323 K. The results are depicted in the plot of  $\log(q_e/C_e)$  vs  $1/T$  (Fig. 8). It is observed that with increase in temperature, the adsorption capacity increases from 56.8 to 58.4 for Pb(II) and 37.1 to 37.7 mg/g for Cd(II), indicating more favourable adsorption at higher temperature and endothermic adsorption process. The high

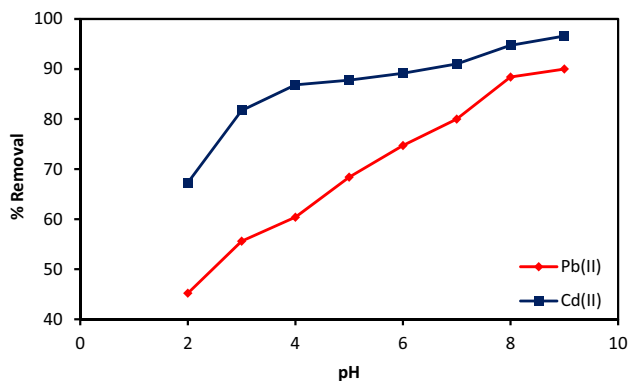


Fig. 7 Effect of pH

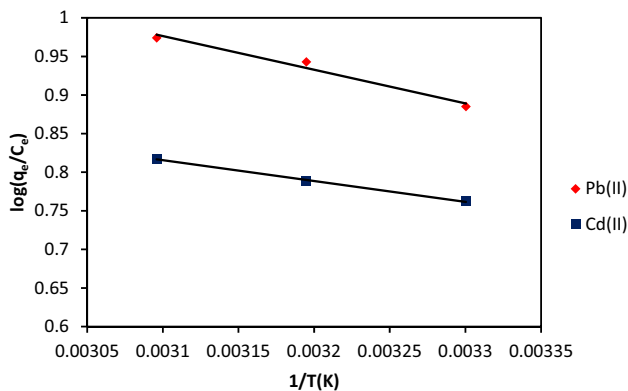


Fig. 8 van't Hoff plots

uptake at higher temperature may be result of increase in (a) adsorbent pore size, (b) affinity of adsorbate towards the adsorbent surface, or (c) driving force to overcome mass transfer resistance of adsorbate between solution and adsorbent surface (Lu et al. 2009).

The thermodynamic parameters such as enthalpy change ( $\Delta H^\circ$ ), and entropy change ( $\Delta S^\circ$ ) were evaluated from the slope and intercept of Fig. 8 using Eq. 4, while Gibbs free energy change ( $\Delta G^\circ$ ) using Eq. 5.

$$\log\left(\frac{q_e}{C_e}\right) = \frac{\Delta S^\circ}{2.303R} - \frac{\Delta H^\circ}{2.303RT} \tag{4}$$

$$\Delta G^\circ = \Delta H^\circ - T\Delta S^\circ \tag{5}$$

where  $T$  is the temperature in Kelvin, and  $R$  is the gas constant (8.314 J/mol/K).

The parameters are tabulated in Table 1. The negative  $\Delta G^\circ$  values suggest spontaneity of the adsorption process. The  $\Delta G^\circ$  values become more and more negative with increasing temperature, reflecting that the adsorption is more favored at higher temperature. The positive values of  $\Delta H^\circ$  and  $\Delta S^\circ$  imply endothermic process and increasing randomness at adsorbate-adsorbent interface.

Table 1 Thermodynamic parameters

Adsorbate	$\Delta H^\circ$ (kJ/mol)	$\Delta S^\circ$ (J/mol/K)	$-\Delta G^\circ$ (kJ/mol)		
			303 K	313 K	323 K
Pb(II)	8.36	44.60	4.42	4.73	5.05
Cd(II)	5.17	31.65	5.16	5.60	6.05

Biosorption isotherms modeling

Langmuir, Freundlich, Temkin and Dubinin–Radushkevich (D–R) isotherm models were used to correlate the experimental data, and to evaluate various isotherm parameters. The values of different parameters along with correlation coefficients ( $R^2$ ) are reported in Table 2.

Langmuir isotherm model suggests monolayer biosorption of adsorbate onto energetically homogenous adsorption sites. The Langmuir isotherm is expressed as:

$$\frac{C_e}{q_e} = \frac{1}{bq_m} + \frac{C_e}{q_m} \tag{6}$$

where  $q_m$  and  $b$  are the maximum monolayer adsorption capacity (mg/g) and Langmuir constant (L/mg). The  $q_m$  and  $b$  were calculated from the slope and intercept of  $C_e/q_e$  vs  $C_e$  plots at 303, 313 and 323 K (Fig. 9). The  $q_m$  for Pb (II) is 100.00 and 72.46 mg/g for Cd(II), which are greater than that for other biosorbents (Table 3), which suggests that epichlorohydrin modified algal biomass is an efficient biosorbent for Pb(II) and Cd(II) removal from industrial effluents. The dimensionless separation parameter ( $R_L$ ), which a measure of favorable adsorption was calculated using Eq. 7:

$$R_L = \frac{1}{(1 + bC_o)} \tag{7}$$

The adsorption is considered unfavorable ( $R_L > 1$ ), favorable ( $0 < R_L < 1$ ), linear ( $R_L = 1$ ) or irreversible ( $R_L = 0$ ). The  $R_L$  values in the range 0.062–0.072 for Pb (II) and 0.042–0.031 for Cd(II) suggests highly favorable adsorption process.

Freundlich adsorption isotherm assumes adsorption on heterogenous surface. The Freundlich isotherm is expressed as:

$$\log q_e = \log k_f + \frac{1}{n_f} \log C_e \tag{8}$$

where  $k_f$  ((mg/g)/(mg/L)<sup>1/n</sup>) is the Freundlich adsorption capacity and  $n_f$  is adsorption intensity. The values of  $k_f$  and  $n_f$  were calculated from the slope and intercept of  $\log q_e$  vs  $\log C_e$  plot (Fig. 10). Lower than unity values of  $1/n_f$  suggest favorable adsorption. The  $1/n_f$  values are 0.36–0.44 for

**Table 2** Various isotherm parameters

Isotherm	Isotherm parameters	Pb(II)			Cd(II)		
		303 K	313 K	323 K	303 K	313 K	323 K
Langmuir	$q_m$	78.74	85.47	100.00	72.46	72.40	71.94
	$b$	0.302	0.288	0.256	0.455	0.526	0.623
	$R_L$	0.062	0.064	0.072	0.042	0.036	0.031
	$R^2$	0.979	0.980	0.984	0.975	0.974	0.973
Freundlich	$k_f$	25.55	25.65	26.00	30.45	32.14	34.04
	$1/n_f$	0.363	0.401	0.437	0.288	0.277	0.265
	$R^2$	0.822	0.871	0.924	0.939	0.927	0.912
Temkin	$K_t$	2.808	2.422	2.221	6.633	8.294	10.862
	$b_t$	144.35	129.45	119.99	196.17	207.17	220.39
	$R^2$	0.877	0.922	0.961	0.926	0.915	0.902
D–R	$q_D$	65.94	68.41	69.88	59.73	60.53	61.33
	$E$	0.707	0.707	0.707	1.000	1.000	1.118
	$R^2$	0.959	0.978	0.978	0.897	0.900	0.902

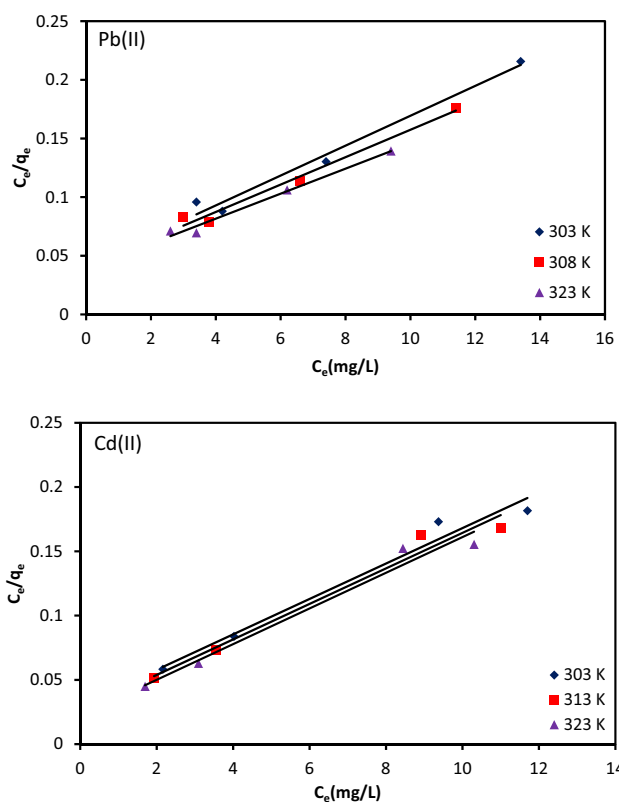


**Fig. 9** Langmuir adsorption isotherm plots

Pb(II) and 0.27–0.29 for Cd(II), which confirm the process to be favorable.

The Temkin isotherm assumes that the heat of adsorption of all the molecules increase linearly with coverage. The isotherm model is expressed as:

$$q_e = (RT/b_t) \ln K_t + (RT/b_t) \ln C_e \tag{9}$$

where  $b_t$  is related to heat of adsorption (J/mol), and  $K_t$  is the equilibrium binding constant (L/g). The values of  $b_t$  and  $K_t$  were calculated from the slope and intercept of  $q_e$  vs  $\ln C_e$  plots (Fig. 11). The values of  $b_t$  between 120 and 220 kJ/mol is indicative of strong interaction between adsorbate and adsorbent surface.

The Dubinin–Radushkevich (D–R) isotherm is applied to estimate the pore filling mechanism and to predict the physical or chemical nature of the adsorption process. The D–R isotherm is expressed as:

$$\ln q_e = \ln q_D - \beta \epsilon^2 \tag{10}$$

where  $q_D$  is the maximum adsorption capacity (mg/g),  $\beta$  is the activity coefficient related to mean sorption energy ( $\text{mol}^2/\text{kJ}^2$ ) and  $\epsilon$  is the Polanyi potential. The values of  $q_D$  and  $\beta$  were calculated from the slope and intercept of linear  $\ln q_e$  vs  $\epsilon^2$  (Fig. 12) plot, whereas  $\epsilon$  value was estimated according to Eq. 11:

$$\epsilon = RT \ln \left( 1 + \frac{1}{C_e} \right) \tag{11}$$

The mean sorption energy ( $E$ ), which is a measure of physical or chemical nature of adsorption, was determined according to Eq. 12:

$$E = \frac{1}{\sqrt{2\beta}} \tag{12}$$

The mean  $E$  values are 0.71 kJ/mol for Pb(II) and 1.0–1.12 kJ/mol for Cd(II), which fall between the range for physical adsorption (0–8 kJ/mol). The less than unity values of  $q_D$  imply surface heterogeneity due to pore structures on the adsorbent surface.

Higher  $R^2$  values (Table 2) is obtained for Langmuir isotherm model, which suggests that the available sites on



**Table 3** Comparison of adsorption capacities ( $q_m$ ) of some reported adsorbents for Pb(II) and Cd(II) removal

Adsorbent	Pb(II)			Cd(II)		
	$q_m$ (mg/g)	pH	Refs.	$q_m$ (mg/g)	pH	Refs.
<i>Euphorbia rigida</i> activated carbon	279.72	–	Geçgel and Gerçel (2007)	329	7	Baláz et al. (2015)
Graphene/c-MWCNTs	104.9	–	Sui et al. (2012)	87.72	8	Pandey and Tiwari (2015)
Epichlorohydrin modified green algal biomass	100.00	5	This work	72.46	6	This work
MnO coated CNTs	78.74	–	Ji et al. (2012)	38.17	7	Khan et al. (2015)
MWCNTs/Fe <sub>3</sub> O <sub>4</sub> nanocomposites modified with 3-aminopropyltriethoxysilane	75.02	5.3	Chun et al. (2013)	35.71	6	Bogusz et al. (2015)
Multiwalled Carbon nanotubes functionalized with tris(2-aminoethyl)-amine	71	5.7–6	Tehrani et al. (2013)	32.57	6	Bogusz et al. (2015)
<i>Pseudomonas aeruginosa</i>	68.4	5.5	Chang et al. (1997)	29.06	5.5	Ghoneim et al. (2014)
$\gamma$ -Alumina	65.67	7	Bhat et al. (2015)	20.41	5–6	Adelagun et al. (2014)
Grape stalks	49.7	5.5	Martínez et al. (2006)	16.13	5.5	Sarada et al. (2014)
Graphene	22.42	4	Huang et al. (2011)	10.86	5	Li et al. (2003)

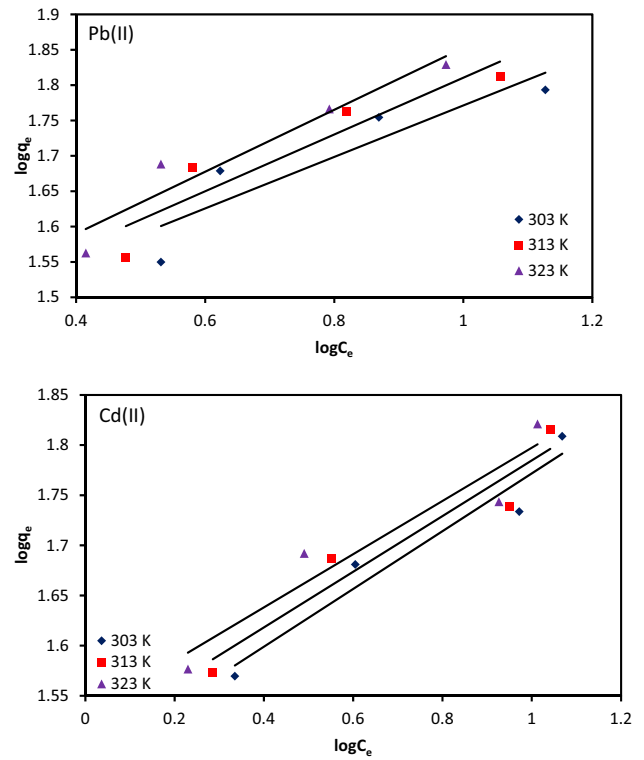


**Fig. 10** Freundlich adsorption isotherm plots

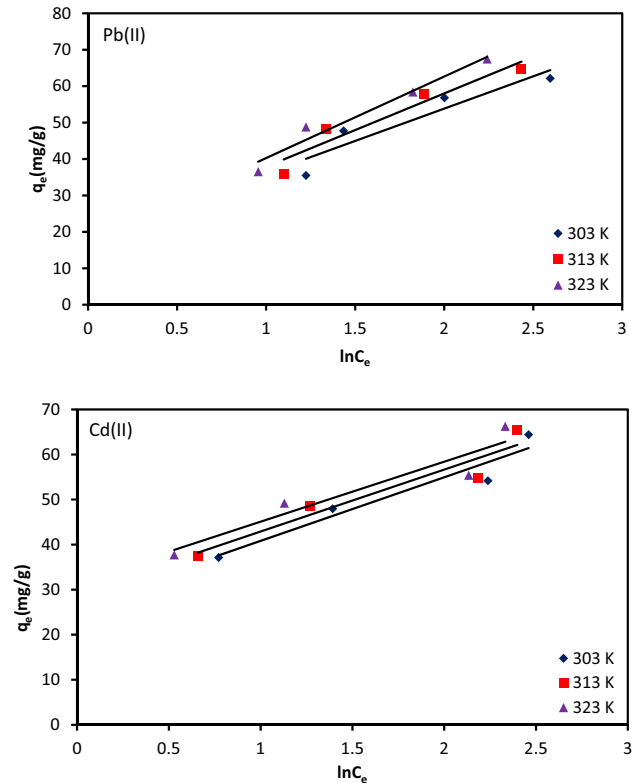


**Fig. 11** Temkin isotherm plots

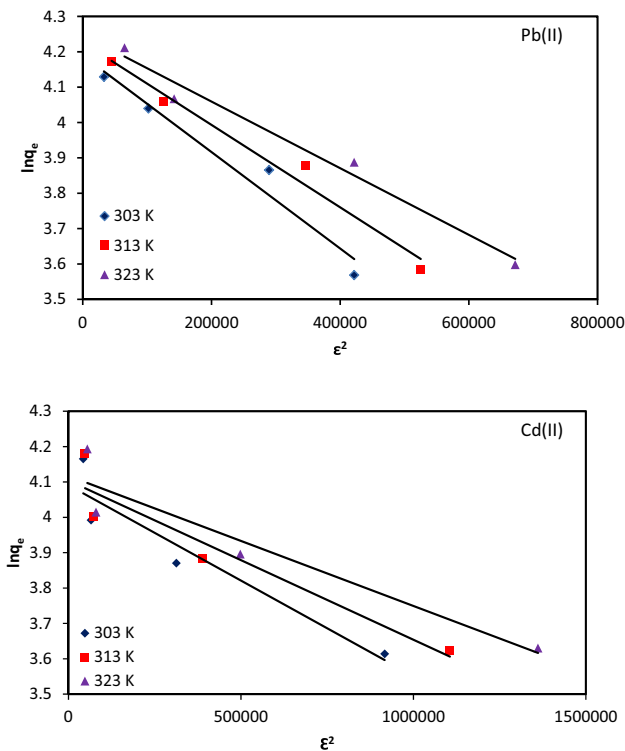


Fig. 12 D-R adsorption isotherm plots

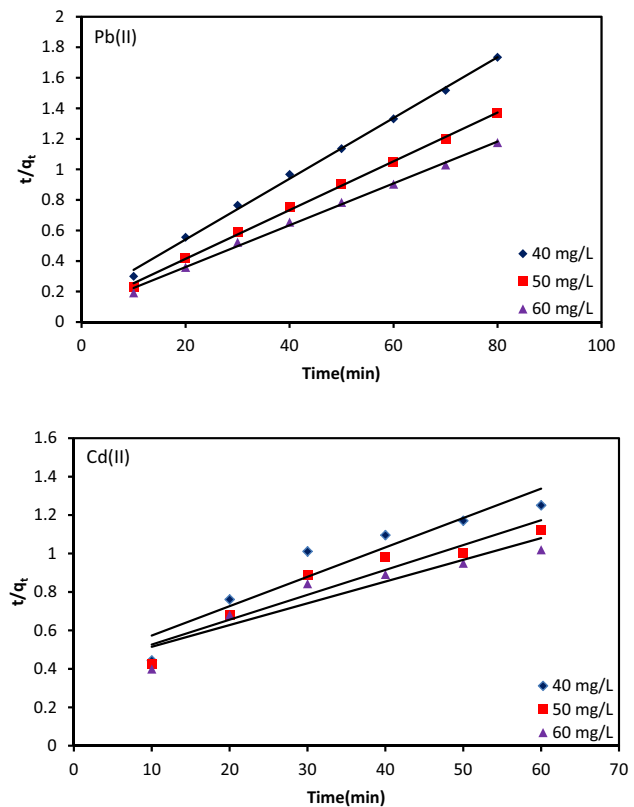


Fig. 14 Pseudo-second order kinetic plots

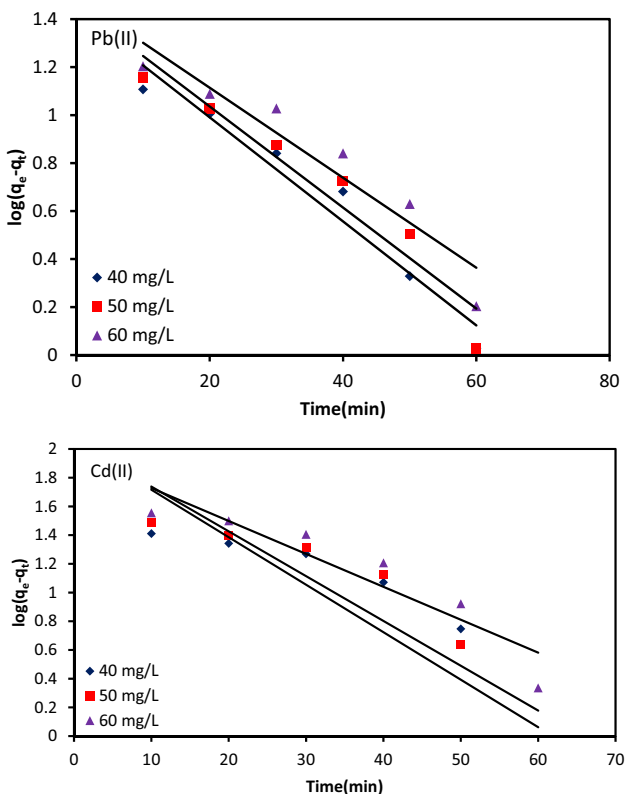


Fig. 13 Pseudo-first order kinetic plots

adsorbent surface are distributed homogenously, and there is monolayer adsorption of both metal ions.

**Biosorption kinetic modeling**

Various kinetic models were used to understand the kinetics of Pb(II) and Cd(II) uptake. The pseudo-first order model implies adsorption of one adsorbate molecule onto one active site, while pseudo-second order model assumes that one adsorbate molecule is adsorbed onto two active sites of the biosorbent.

The pseudo-first order and pseudo-second order models are expressed as:

$$\log(q_e - q_t) = \log q_e - \frac{k_1 \cdot t}{2.303} \tag{13}$$

$$\frac{t}{q_t} = \frac{1}{(k_2 q_e^2)} + \frac{t}{q_e} \tag{14}$$

where  $q_t$  (mg/g), is the amount of metal ions adsorbed at time  $t$ ,  $k_1$  and  $k_2$  are the pseudo-first order (1/min) and pseudo-second order rate (g/mg/min) constants. The values of  $q_e$  and the rate constants were calculated from the plots  $\log(q_e - q_t)$  vs  $t$  (Fig. 13) and  $t/q_t$  vs  $t$  (Fig. 14), which are reported in Table 4 along with  $R^2$ . The higher  $R^2$  values

**Table 4** Pseudo-first order, pseudo-second order, liquid film and intraparticle diffusion model parameters

Adsorbate	Conc (mg/L)	Pseudo-first order			$q_e(exp)$	Pseudo-second order			Liquid film diffusion		Intraparticle diffusion	
		$k_f(1/min)$	$q_e(cal)$ (mg/g)	$R^2$		$k^2 \times 10^{-2}$ (g/mg/min)	$q_e(cal)$ (mg/g)	$R^2$	$k_D$	$R^2$	$K_i$	$R^2$
Pb(II)	40	0.4997	22.12	0.954	46.13	0.352	46.72	0.998	0.0499	0.954	2.007	0.977
	50	0.4836	23.85	0.927	58.40	0.342	59.17	0.998	0.0485	0.927	2.195	0.984
	60	0.4329	25.69	0.907	68.00	0.278	69.93	0.997	0.0432	0.907	2.506	0.982
Cd(II)	40	0.0762	111.40	0.728	48.27	0.057	64.10	0.896	0.0762	0.729	5.645	0.947
	50	0.0718	112.46	0.818	54.17	0.031	88.49	0.895	0.0719	0.818	6.792	0.963
	60	0.0527	90.63	0.801	60.99	0.041	77.51	0.906	0.0528	0.861	7.669	0.957

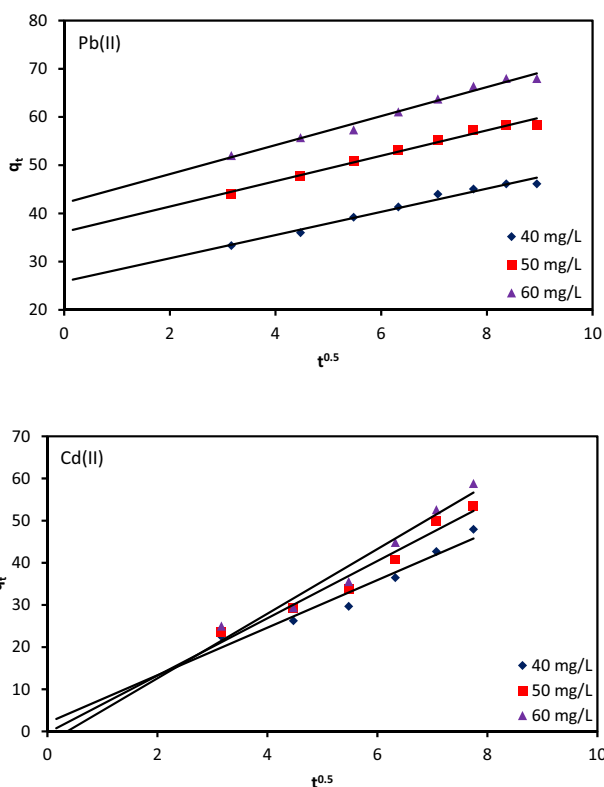


**Fig. 15** Intraparticle diffusion plots

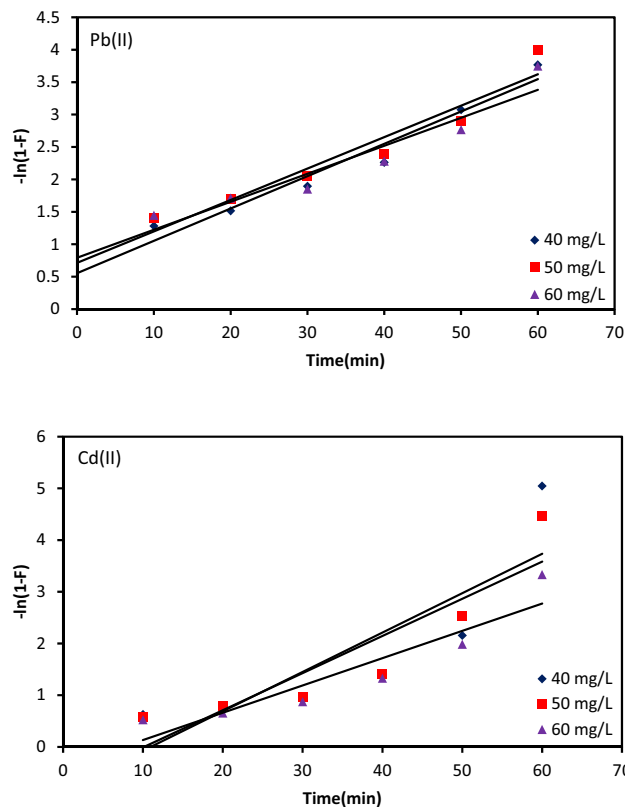


**Fig. 16** Liquid film diffusion plots

suggest that pseudo-second order kinetics is more suitable to explain the experimental data.

The mechanism of adsorption was determined by applying Weber–Moris and Boyd model as:

$$q_t = k_i \cdot t^{0.5} + C_i \tag{15}$$

$$-\ln\left(1 - \frac{q_t}{q_e}\right) = k_{fd} \cdot t \tag{16}$$

where  $k_i$  (mg/g min<sup>0.5</sup>) is intraparticle diffusion rate constant,  $C_i$  is a constant (mg/g) which gives an idea about the thickness of the boundary layer on the adsorbent surface,

$k_{fd}$  (1/min) is the film diffusion rate constant, and  $F$  is the fractional attainment of equilibrium ( $F = q_t/q_e$ ) at time  $t$ .

It is considered that a multilinear  $q_t$  vs  $t^{0.5}$  plot passing through the origin is indicative of the intraparticle diffusion to be the sole rate limiting step, whereas a straightline plot of  $-\ln(1-q_t/q_e)$  vs  $t$  with zero intercept suggests that the adsorption is controlled by film diffusion. The intraparticle diffusion plots, are not multilinear and do not pass through the origin in case of Pb(II) and Cd(II) adsorption, therefore it may not be considered as the sole rate controlling step (Fig. 15). However, film diffusion plots of Pb(II) almost passes through the origin suggesting that the film diffusion

is rate controlling (Fig. 16). Intraparticle and film diffusion may be the rate controlling steps in case of Cd(II) adsorption.

## Conclusions

The green algae modified with epichlorohydrin efficiently removes Pb(II) and Cd(II) from aqueous solution. The adsorption process variables (contact time, dose, initial metal ion concentration, initial solution pH, and temperature) have been optimized. A strong correlation between the data and Langmuir model suggests that the adsorbent has homogenous distribution of surface energy thereby inducing monolayer adsorption. Pseudo-second order kinetics model properly describes the adsorption kinetics of both the metal ions. The mechanism of adsorption of Pb(II) is controlled by film diffusion. Intraparticle and film diffusion may be the rate controlling steps in case of Cd(II) adsorption. The thermodynamics studies suggest the adsorption process to be spontaneous, endothermic and entropy driven.

## References

- Abdel-Aty AM, Ammar NS, Abdel Ghafar HH, Ali RK (2013) Biosorption of cadmium and lead from aqueous solution by fresh water alga *Anabaena sphaerica* biomass. *J Adv Res* 4:367–374
- Adelagun ROA, Itodo AU, Berezi EP, Oko OJ, Kamba EA, Andrew C, Bello HA (2014) Adsorptive removal of Cd<sup>2+</sup> and Zn<sup>2+</sup> from aqueous system by BSG. *Chem Mater Res* 6:104–112
- Akbari M, Hallajisani A, Reza KA, Shahbeig H, Ghorbanian SA (2015) Equilibrium and kinetic study and modeling of Cu(II) and Co(II) synergistic biosorption from Cu(II)–Co(II) single and binary mixtures on brown algae *C. indica*. *J Environ Chem Eng* 3:140–149
- Ali I, Khan TA, Asim M (2012) Removal of arsenate from groundwater by electrocoagulation method. *Environ Sci Pollut Res* 19:1668–1676
- Anastopoulos I, Kyzas GZ (2015) Progress in batch biosorption of heavy metals onto algae. *J Mol Liq* 209:77–86
- Areco MM, Hanela S, Duran J, Afonso Mdos S (2012) Biosorption of Cu(II), Zn(II), Cd(II) and Pb(II) by dead biomasses of green alga *Ulva lactuca* and the development of a sustainable matrix for adsorption implementation. *J Hazard Mater* 213–214:123–132
- Baláz M, Bujňáková Z, Baláz P, Zorkovská A, Danková Z, Briánčin J (2015) Adsorption of cadmium(II) on waste biomaterial. *J Colloid Interface Sci* 454:121–133
- Bhat A, Megeri GB, Thomas C, Bhargava H, Jeevitha C, Chandrashekhara S, Madhu GM (2015) Adsorption and optimization studies of lead from aqueous solution using  $\gamma$ -Alumina. *J Environ Chem Eng* 3:30–39
- Bogusz A, Oleszczuk P, Dobrowolski R (2015) Application of laboratory prepared and commercially available biochars to adsorption of cadmium, copper and zinc ions from water. *Bioresour Technol* 196:540–549
- Carlsson AS, van Beilen J, Möller R, Clayton D (2003) Micro- and macro-algae: utility for industrial applications. CPL Press, New York
- Chang J, Law R, Chang C (1997) Biosorption of lead, copper and cadmium by biomass of *Pseudomonas aeruginosa* PU21. *Water Res* 31:1651–1658
- Chojnacka K, Chojnacki A, Górecka H (2005) Biosorption of Cr<sup>3+</sup>, Cd<sup>2+</sup> and Cu<sup>2+</sup> ions by blue-green algae *Spirulina sp.*: Kinetics, equilibrium and the mechanism of the process. *Chemosphere* 59:75–84
- Chun K, Moon I, Han J, Do S, Lee J, Jeon S (2013) Highly water-soluble multi-walled carbon nanotubes amine-functionalized by supercritical water oxidation. *Nanoscale* 5:10171–10174
- Cooper J, Bolbot JA, Saini S, Setford SJ (2007) Electrochemical method for the rapid on site screening of cadmium and lead in soil and water samples. *Water Air Soil Pollut* 179:183–195
- Crist RH, Oberholser K, Shank N, Nguyen M (1981) Nature of bonding between metallic ions and algal cell walls. *Environ Sci Technol* 15:1212–1217
- Dąbrowski A, Hubicki Z, Podkościelny P, Robens E (2004) Selective removal of the heavy metal ions from waters and industrial wastewaters by ion-exchange method. *Chemosphere* 56:91–106
- El-Samrani AG, Lartiges BS, Villieras F (2008) Chemical coagulation of combined sewer overflow: Heavy metal removal and treatment optimization. *Water Res* 42:951–960
- Ferreira LS, Rodrigues MS, de Carvalho JCM, Lodi A, Finocchio E, Perego P, Converti A (2011) Adsorption of Ni<sup>2+</sup>, Zn<sup>2+</sup> and Pb<sup>2+</sup> onto dry biomass of *Arthrospira (Spirulina) platensis* and *Chlorella vulgaris*. I. Single metal systems. *Chem Eng J* 173:326–333
- Freitas OM, Martins RJ, Delerue-Matos CM, Boaventura RA (2008) Removal of Cd(II), Zn(II) and Pb(II) from aqueous solutions by brown marine macro algae: Kinetic modelling. *J Hazard Mater* 153:493–501
- Gerçel Ö, Gerçel HF (2007) Adsorption of lead(II) ions from aqueous solutions by activated carbon prepared from biomass plant material of *Euphorbia rigida*. *Chem Eng J* 132(2007):289–297
- Ghoneim MM, El-Desoky HS, El-Moselhy KM, Amer A, El-Naga EH, Mohamedein LI, Al-Prol AE (2014) Removal of cadmium from aqueous solution using marine green algae, *Ulva lactuca*. *Egypt J Aqu Res* 40:235–242
- Göksungur Y, Üren S, Güvenç U (2005) Biosorption of cadmium and lead ions by ethanol treated waste baker's yeast biomass. *Bioresour Technol* 96:103–109
- Haltunen T, Salminen S, Tahvonen R (2007) Rapid removal of lead and cadmium from water by specific lactic acid bacteria. *Int J Food Microbiol* 114:30–35
- Han R, Li H, Li Y, Zhang J, Xiao H, Shi J (2006) Biosorption of copper and lead ions by waste beer yeast. *J Hazard Mater* B137:1569–1576
- He J, Chen JP (2014) A comprehensive review on biosorption of heavy metals by algal biomass: Materials, performances, chemistry, and modeling simulation tools. *Bioresour Technol* 160:67–78
- Hu Y-R, Guo C, Wang F, Wang S-K, Pan F, Liu C-Z (2014) Improvement of microalgae harvesting by magnetic nanocomposites coated with polyethylenimine. *Chem Eng J* 242:341–347
- Huang ZH, Zheng X, Lv W, Wang M, Yang QH, Kang F (2011) Adsorption of lead (II) ions from aqueous solution on low-temperature exfoliated graphene nanosheets. *Langmuir* 27:7558–7562
- Ivánová D, Kaduková J, Kavuličová J, Horváthová H (2012) Determination of the functional groups in algae *Parachlorella kessleri* by potentiometric titrations. *Nova Biotechnol Chim* 11:93–99
- Javadian H, Ahmadi M, Ghiasvand M, Kahrizi S, Katald R (2013) Removal of Cr(VI) by modified brown algae *Sargassum bevanom* from aqueous solution and industrial wastewater. *J Taiwan Inst Chem Eng* 44:977–989

- Jayakumar R, Rajasimman M, Karthikeyan C (2014) Sorption of from aqueous solution using marine green algae *Halimeda gracilis*: Optimization, equilibrium, kinetic, thermodynamic and desorption studies. *J Environ Chem Eng* 2:1261–1274
- Jayakumar R, Rajasimman M, Karthikeyan C (2015) Optimization, equilibrium, kinetic, thermodynamic and desorption studies on the sorption of Cu(II) from an aqueous solution using marine green algae: *Halimeda gracilis*. *Ecotoxicol Environ Saf* 121:199–210
- Ji L, Zhou L, Bai X, Shao Y, Zhao G, Qu Y, Wang C, Li Y (2012) Facile synthesis of multiwall carbon nanotubes/iron oxides for removal of tetrabromobisphenol A and Pb(II). *J Mater Chem* 22:15853–15862
- Kapoor A, Viraraghavan T, Cullimore DR (1999) Removal of heavy metals using the fungus *Aspergillus niger*. *Bioresour Technol* 70:95–104
- Khan TA, Singh VV (2010) Removal of cadmium (II), lead (II), and chromium (VI) ions from aqueous solution using clay. *Toxicol Environ Chem* 92:1435–1446
- Khan TA, Dahiya S, Ali I (2012) Removal of direct red 81 dye from aqueous solution by native and citric acid modified bamboo sawdust-Kinetic study and equilibrium isotherm analyses. *G U J Sci* 25:59–87
- Khan TA, Sharma S, Khan EA, Mukhlif AA (2014) Removal of congo red and basic violet 1 by chir pine (*Pinus roxburghii*) sawdust, a saw mill waste: Batch and column studies. *Toxicol Environ Chem* 96:555–568
- Khan TA, Nazir M, Khan EA (2015) Magnetically modified multiwalled carbon nanotubes for the adsorption of bismarck brown R and Cd(II) from aqueous solution: Batch and column studies. *Desal Water Treat*. doi:10.1080/19443994.2015.1100553
- Kratochvil D, Pimentel P, Volesky B (1998) Removal of trivalent and hexavalent chromium by seaweed biosorbent. *Environ Sci Technol* 32:2693–2698
- Ku Y, Jung IL (2001) Photocatalytic reduction of Cr(VI) in aqueous solutions by UV irradiation with the presence of titanium dioxide. *Water Res* 35:135–142
- Li Y-H, Ding J, Luan Z, Di Z, Zhu Y, Xu C, Wu D, Wei B (2003) Competitive adsorption of Pb, Cu and Cd ions from aqueous solutions by multiwalled carbon nanotubes. *Carbon* 41:2787–2792
- Liu Y, Cao Q, Luo F, Chen J (2009) Biosorption of Cd<sup>2+</sup>, Cu<sup>2+</sup>, Ni<sup>2+</sup> and Zn<sup>2+</sup> ions from aqueous solutions by pretreated biomass of brown algae. *J Hazard Mater* 163:931–938
- Loaic M, Olier R, Guezennec J (1997) Uptake of lead, cadmium and zinc by a novel bacterial exopolysaccharide. *Water Res* 31:1171–1179
- Lou Z, Wang J, Jin X, Wan L, Wang Y, Chen H, Shan W, Xiong Y (2015) Brown algae based new sorption material for fractional recovery of molybdenum and rhenium from wastewater. *Chem Eng J* 273:231–239
- Lu D, Cao Q, Cao X, Luo F (2009) Removal of Pb(II) using modified lawn grass: Mechanism, kinetics, equilibrium and thermodynamic studies. *J Hazard Mater* 166:239–247
- Martínez M, Miralles N, Hidalgo S, Fiol N, Villaescusa I, Poch J (2006) Removal of lead (II) and cadmium (II) from aqueous solutions using grape stalk waste. *J Hazard Mater* 133:203–211
- Martins RJE, Pardo R, Boaventura RAR (2004) Cadmium (II) and zinc (II) adsorption by the aquatic moss *Fontinalis antipyretica*: Effect of temperature, pH and water hardness. *Water Res* 38:693–699
- Mohan S, Sreelakshmi G (2008) Fixed bed column study for heavy metal removal using phosphate treated rice husk. *J Hazard Mater* 153:75–82
- Montazer-Rahmatia MM, Rabbania P, Abdolalia A, Keshtkar AR (2011) Kinetics and equilibrium studies on biosorption of cadmium, lead, and nickel ions from aqueous solutions by intact and chemically modified brown algae. *J Hazard Mater* 185:401–407
- Pandey S, Tiwari S (2015) Facile approach to synthesize chitosan based composite—characterization and cadmium(II) ion adsorption studies. *Carbohydr Polym* 134:646–656
- Sadrzadeh M, Mohammadi T, Ivakpour J, Kasiri N (2008) Separation of lead ions from wastewater using electro dialysis: Comparing mathematical and neural network modelling. *Chem Eng J* 144:431–441
- Sar A, Tuzen M (2008a) Biosorption of cadmium(II) from aqueous solution by red algae (*Ceramium virgatum*): Equilibrium, kinetic and thermodynamic studies. *J Hazard Mater* 157:448–454
- Sar A, Tuzen M (2008b) Biosorption of total chromium from aqueous solution by red algae (*Ceramium virgatum*): Equilibrium, kinetic and thermodynamic studies. *J Hazard Mater* 160:349–355
- Sar A, Tuzen M (2009) Equilibrium, thermodynamic and kinetic studies on aluminum biosorption from aqueous solution by brown algae (*Padina pavonica*) biomass. *J Hazard Mater* 171:973–979
- Sarada B, Prasad KM, Kumar KK, Murthy ChVR (2014) Cadmium removal by macro algae *Caulerpa fastigiata*: characterization, kinetic, isotherm and thermodynamic studies. *J Environ Chem Eng* 2:1533–1542
- Sui Z, Meng Q, Zhang X, Ma R, Cao B (2012) Green synthesis of carbon nanotube–graphene hybrid aerogels and their use as versatile agents for water purification. *J Mater Chem* 22:8767–8771
- Teemu H, Seppo S, Jussi M, Raija T, Kalle L (2008) Reversible surface binding of cadmium and lead by lactic acid and bifidobacteria. *Int J Food Microb* 125:170–175
- Tehrani MS, Azar PA, Namin PE, Dehaghi SM (2013) Removal of lead ions from wastewater using functionalized multiwalled carbon nanotubes with tris(2-aminoethyl)amine. *J Environ Prot* 4:529–536
- Tuzen M, Sari A, Mendil D, Uluzlu OD, Soylak M, Dogan M (2009) Characterization of biosorption process of As(III) on green algae *Ulothrix cylindricum*. *J Hazard Mater* 165:566–572
- Yang J, Volesky B (1999) Modeling uranium-proton ion exchange in biosorption. *Environ Sci Technol* 33:4079–4085